

Modeling the composition of Au-catalyzed $\text{InP}_x\text{As}_{1-x}$ and $\text{InSb}_x\text{As}_{1-x}$ nanowires

© E.D. Leshchenko¹, V.G. Dubrovskii²

¹ Submicron Heterostructures for Microelectronics, Research & Engineering Center, RAS, St. Petersburg, Russia

² St. Petersburg State University, St. Petersburg, Russia

E-mail: leshchenko.spb@gmail.com

Received September 4, 2025

Revised September 17, 2025

Accepted September 17, 2025

The formation of Au-catalyzed $\text{InP}_x\text{As}_{1-x}$ and $\text{InSb}_x\text{As}_{1-x}$ nanowires has been studied theoretically. Taking into account the desorption, we have studied the influence of the III/V flux ratio and temperature on the nanowire composition. Using the Au-catalyzed $\text{InP}_x\text{As}_{1-x}$ nanowires as an example, we have shown that the Au concentration has no effect on the vapor–solid distribution but affects the total concentration of group V elements. The study has shown that the total concentration of group V elements is low (about 1–2%). Comparison of the theoretical results with available experimental data have demonstrated a good agreement.

Keywords: modeling, III–V nanowires, chemical composition, ternary compounds.

DOI: 10.61011/TPL.2026.01.62830.20489

Despite more than 30 years of research into nanowires (NWs), the intensity of work in this area remains quite high. One of the NW advantages is efficient relaxation of elastic stresses on the lateral surface [1] (and, hence, the possibility of combining different materials without defect formation). In addition, growth of NWs is characterized by a high degree of control over all parameters, including crystal structure [2], radius [3], length [4], location [5], doping level [6], and chemical composition [7]. Most NWs are being grown via the vapor–liquid–solid mechanism; as a catalyst, gold is often used [8]. In the case when the droplet consists of a metal that is part of NW (e.g. In), the self-catalyzed growth takes place [9]. Among the popular synthesis methods, metal-organic vapor-phase epitaxy (MOVPE) [10] and molecular beam epitaxy [11] may be distinguished.

NW research is mainly focused on, e.g., compositional control of ternary nanostructures [12], which is necessary to create optoelectronic devices [13]. For a long time, most theoretical studies were aimed at examining the NW composition dependence on the droplet composition (i.e., the liquid–solid distribution) [14]. Depending on the mode of atom incorporation, models are divided into equilibrium [15], nucleation-limited [16] and kinetic [17]. However, except for the case of *in situ* studying the growth of $\text{In}_x\text{Ga}_{1-x}\text{As}$ NW by transmission electron microscopy [18], the final result of the experiment is the NW composition dependence on the gas phase one (i.e., the vapor–solid distribution) [12]. In most cases, such dependences were described by the one-parameter Langmuir–McLean equation [19]. An important milestone was publication [20] which presented a generalized model combining kinetics and thermodynamics and showed how the kinetic distribution is being shifted to equilibrium one with increasing

flux ratio (e.g., V/III for the III–V–V systems). This was followed by a whole series of studies [21–23] aimed at more detailed analysis and elimination of uncertainties associated with the liquid. Paper [23] presents a complete model; however, the analysis was performed in this study based on a simplified solution. This paper is devoted to studying formation of the Au-catalyzed $\text{InP}_x\text{As}_{1-x}$ and $\text{InSb}_x\text{As}_{1-x}$ NWs. In contrast to [23], we have calculated the vapor–solid compositional dependence via a complete model taking into account the desorption and interatomic interactions in the droplet. This makes it possible to estimate a number of parameters, including the total concentration of group V elements, and to assess the effect of gold concentration on the vapor–solid distribution and total concentration of group V elements.

Consider the formation of ternary NWs from a supersaturated four-component droplet containing elements *A*, *B* and *C*, and gold as a catalyst. In this paper, *A* and *B* denote group V elements, while *C* denotes a group III element. As shown in publications [21–23], the liquid–solid distribution has the following form:

$$y = \frac{x + g(x)}{x + c_l(1 - x)}, \quad (1)$$

$$g(x) = \Gamma_l x(1 - x) [c_l e^{\omega(1-x)^2} - \beta_l e^{\omega x^2}], \quad (2)$$

$$\Gamma_l = \frac{1}{\chi_{tot} \mathcal{K}} e^{-\Delta \mu_{AC}^0 - \psi_A - \psi_C}. \quad (3)$$

Here x is the $A_x B_{1-x} C$ NW composition, $y = \chi_A / (\chi_A + \chi_B)$, where $\chi_j = N_j / N_{tot}$ denotes the concentration of element *j* atoms in the droplet expressed as a fraction of unity, N_j is the number of element *j* atoms in the droplet, N_{tot} is the total number of atoms in the droplet, ω is the parameter of interaction between pairs *AC* and *BC*

in the solid solution. The formulae involve quantities $c_l = (D_A/D_B)e^{\psi_A-\psi_B}$ and $\beta_l = e^{\Delta\mu_{AC}^0-\Delta\mu_{BC}^0+\psi_A-\psi_B}$, where D_A and D_B are the diffusion coefficients of atoms of elements A and B in the droplet consisting of element C . Function ψ_j describes interatomic interactions in the droplet according to expression $\mu_j^l = \mu_j^{l,0} + \ln\chi_j + \psi_j$, where μ_j^l is the chemical potential of element j in the four-component droplet, $\mu_j^{l,0}$ is the chemical potential of element j in the liquid phase. Here $\Delta\mu_{AC}^0 = \mu_A^{l,0} + \mu_C^{l,0} - \mu_{AC}^{s,0}$ and $\Delta\mu_{BC}^0 = \mu_B^{l,0} + \mu_C^{l,0} - \mu_{BC}^{s,0}$, where $\mu_{AC}^{s,0}$ and $\mu_{BC}^{s,0}$ are the chemical potentials of pairs AC and BC in the crystalline phase, respectively. Values of interaction parameters and chemical potentials necessary to calculate chemical potentials and desorption rate may be found in [24]. Next, total concentration of group V elements $\chi_{tot} = \chi_A + \chi_B$ may be represented as in [23]:

$$\chi_{tot}^2 = \frac{\varepsilon - 1}{K[y^2 + \xi(1-y)^2]}. \quad (4)$$

If we consider the stationary growth mode described as $x\sigma_C I_C = 2\sigma_A I_A - I_A^{des}$ and $(1-x)\sigma_C I_C = 2\sigma_B I_B - I_B^{des}$ [22], where I_A^{des} and I_B^{des} are the desorption fluxes of elements A and B , respectively, it is possible to express the vapor–solid distribution as follows:

$$z = \frac{x}{\varepsilon} + \left[1 - \frac{1}{\varepsilon}\right] \frac{1}{1 + \xi[(1-y)/y]^2}, \quad (5)$$

$$\varepsilon = \frac{2\sigma_5(I_{A_2} + I_{B_2})}{\sigma_C I_C}, \quad \xi = \frac{I_{B_2}^0 e^{2(\psi_B - \psi_A)}}{I_{A_2}^0}, \quad K = \frac{2\sigma_5 I_{A_2}^0 e^{2\psi_A}}{\sigma_C I_C}. \quad (6)$$

Here $I_{A_2}^0$ and $I_{B_2}^0$ are the fluxes of dimers A_2 and B_2 which are in equilibrium with pure liquids A and B , respectively; I_{A_2} , I_{B_2} and I_C are the gaseous fluxes of dimers A_2 , B_2 and atoms C into the droplet; σ_5 and σ_C are the geometric coefficients depending on the contact angle; $z = I_{A_2}/(I_{A_2} + I_{B_2})$ is the gas phase composition.

Let us start the analysis by comparing theoretical results obtained via the complete model and via the approximate solution. As the model system, Au-catalyzed NWs $\text{InP}_x\text{As}_{1-x}$ were chosen. Approximate solution of (1) implies that $g(x) = 0$ (this is primarily due to the value of $\Delta\mu_{AC}^0$), i.e. $y(x)$ is replaced with the kinetic one-parameter distribution

$$y_{kin} = \frac{x}{x + c_l(1-x)}. \quad (7)$$

The compositional dependences obtained for $T = 390$, 450 and 500°C , $\chi_{Au} = 0.58$, $\varepsilon = 4$, $\sigma_5/\sigma_C = 0.03$, $D_P/D_{As} = 0.1$ and $I_C = 1 \text{ ML/s}$ (ML is monolayer) are shown in Fig. 1. Evidently, the selected parameters and temperatures optimal for growing the $\text{InP}_x\text{As}_{1-x}$ NWs provide the approximate solution close to the exact one. The discrepancy between the exact and approximate solutions is observed only at high temperatures $T = 500^\circ\text{C}$. Note that the approximate solution depends on temperature only slightly.

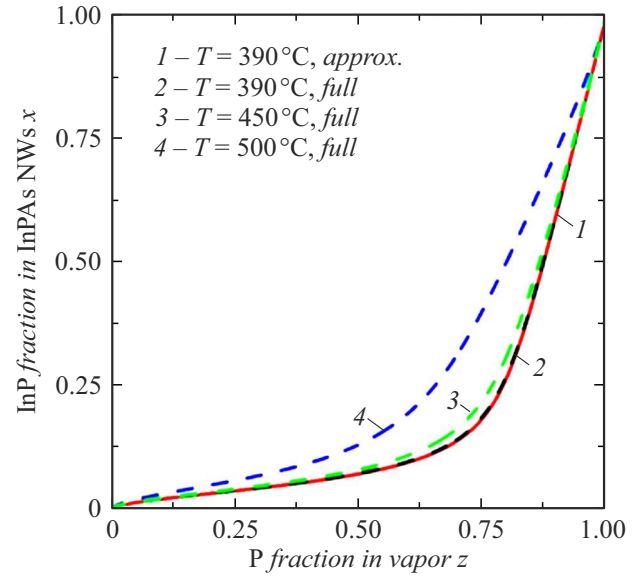


Figure 1. Model vapor–solid distributions for Au-catalyzed NWs $\text{InP}_x\text{As}_{1-x}$ calculated based on the approximate and complete models. The compositional dependences were obtained at $\chi_{Au} = 0.58$, $\varepsilon = 4$, $\sigma_5/\sigma_C = 0.03$, $D_P/D_{As} = 0.1$ and $I_C = 1 \text{ ML/s}$, $T = 390$, 450 and 500°C .

Now let us analyze the growth of the Au-catalyzed $\text{InP}_x\text{As}_{1-x}$ NWs obtained in [25]. These nanostructures were grown at different temperatures by chemoepitaxy using Au-droplets $R^{Au} = 25 \text{ nm}$ in radius. The NW diameter was $R^{NW} = 30 \pm 2.5 \text{ nm}$. Knowing the ratio between the droplet volumes, it is possible to estimate χ_{Au} . Assuming that the contact angle remains constant, obtain $\chi_{Au} \approx R^{Au}/R^{NW} = 0.58$. Fig. 2 presents the compositional dependences obtained at $\sigma_5/\sigma_C = 0.03$, $\varepsilon = 4$, $I_C = 1 \text{ ML/s}$ and $D_P/D_{As} = 0.1, 0.2$ and 0.3 at $T = 390, 405$ and 435°C , respectively. It is evident that an increase in temperature leads to an increase in the efficiency of P atoms incorporation. Fig. 2, *b* presents the χ_{tot} dependence on the gas composition; for the solid lines, the same parameters as in Fig. 2, *a* are used. We can see that the total concentration of group V atoms is low (about 1–2%). Decrease in σ_5/σ_C (down to 0.1) results in a decrease in χ_{tot} . The dashed line corresponds to $\chi_{Au} = 0.5$. One can see that χ_{Au} affects χ_{tot} ; however, $x(z)$ depends on χ_{Au} only slightly.

Finally, let us consider the influence of flux ratio V/III on the formation of nanostructures by using for example the analysis of growth of Au-catalyzed NWs $\text{InSb}_x\text{As}_{1-x}$ [26]. In [26], NWs $\text{InSb}_x\text{As}_{1-x}$ were grown from Au droplets 50 nm in diameter by the MOVPE method using precursors TMIIn, TMSb and AsH_3 . In calculation, we assumed that $\chi_{Au} = 0.15$ which corresponds to the NW diameter of 95 nm . NWs were grown at $T = 450^\circ\text{C}$ and flux ratios $V/III = 15$ of 27 and 56 . When $V/III = 15$, $x \approx z$ which should correspond to $\varepsilon = 1$; therefore, $\sigma_5/\sigma_C = 0.03$. Then $\varepsilon = 1.6$ and 3.4 for $V/III = 27$ and 56 , respectively. Fig. 3 presents the compositional dependences for different

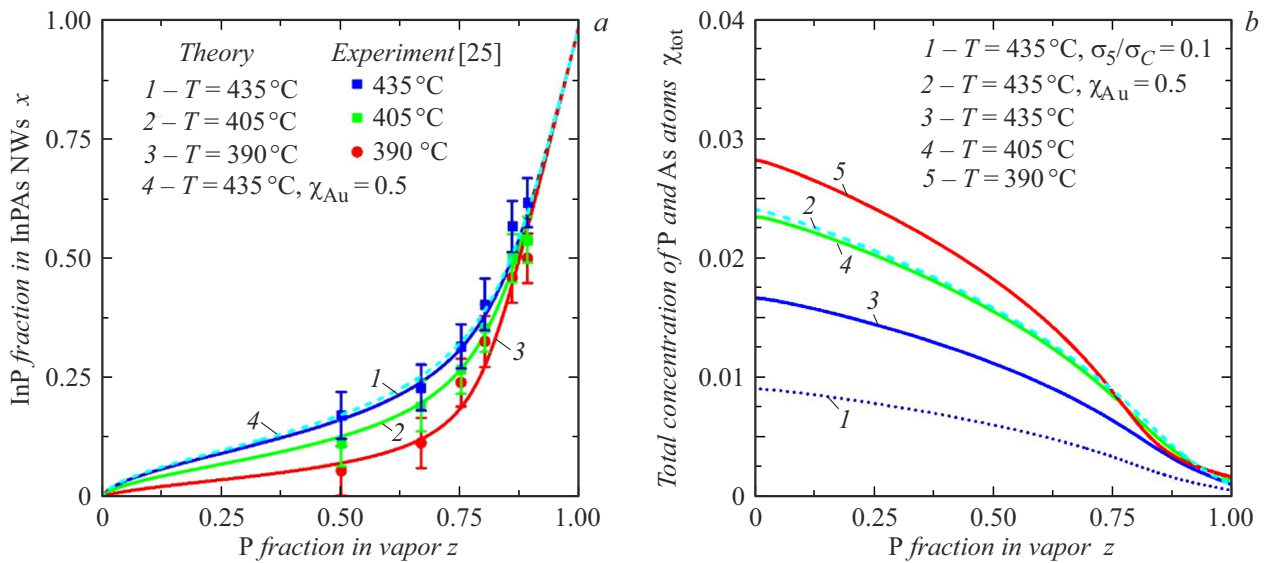


Figure 2. *a* — experimental [25] and theoretical vapor–solid distributions for the Au-catalyzed $\text{InP}_x\text{As}_{1-x}$ NWs at various temperatures. Solid curves were obtained for $\chi_{\text{Au}} = 0.58$, $\sigma_5/\sigma_C = 0.03$, $\varepsilon = 4$, $I_C = 1 \text{ ML/s}$ and $D_P/D_{\text{As}} = 0.1, 0.2$ and 0.3 at $T = 390, 405$ and 435°C . The dashed line was obtained at $T = 435^\circ\text{C}$, $D_P/D_{\text{As}} = 0.3$ and $\chi_{\text{Au}} = 0.5$. *b* — total concentration of the group V atoms versus gas composition for the Au-catalyzed $\text{InP}_x\text{As}_{1-x}$ NWs. The dotted line corresponds to $T = 435^\circ\text{C}$, $D_P/D_{\text{As}} = 0.3$ and $\sigma_5/\sigma_C = 0.1$.

ε and fixed $D_{\text{Sb}}/D_{\text{As}} = 0.001$, $I_C = 1 \text{ ML/s}$. As shown, flux ratio V/III (and, hence, ε) affects the curve shape: $x \approx z$ at $\varepsilon = 1$, while at $\varepsilon = 3.4$ the curve is nonlinear, which indicates more efficient incorporation of As.

Thus, we have theoretically studied the formation of the Au-catalyzed $\text{InP}_x\text{As}_{1-x}$ and $\text{InSb}_x\text{As}_{1-x}$ NWs by using a model involving desorption and influence of the droplet. In the simplified model, atomic concentrations are not taken

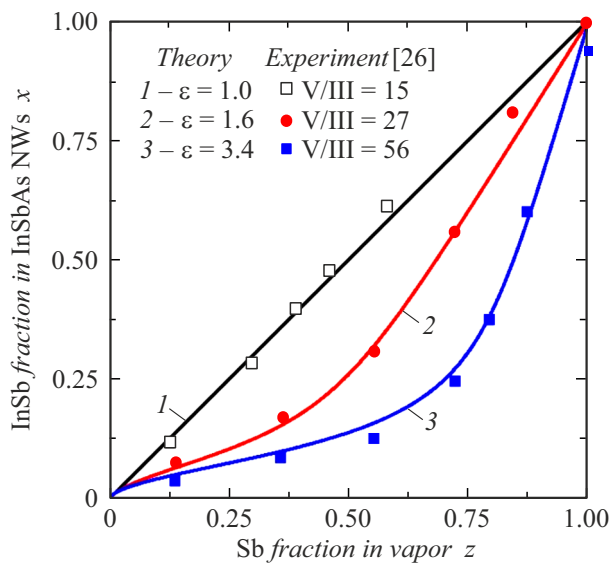


Figure 3. Experimental [26] and theoretical vapor–solid distributions for the $\text{InSb}_x\text{As}_{1-x}$ NWs at different flux ratios V/III . The compositional dependences were obtained at $D_{\text{Sb}}/D_{\text{As}} = 0.001$, $I_C = 1 \text{ ML/s}$, $\varepsilon = 1, 1.6$ and 3.4 , $T = 450^\circ\text{C}$, $\sigma_5/\sigma_C = 0.03$, $\chi_{\text{Au}} = 0.15$.

into account in calculating $z(x)$ and, hence, interactions within the droplet (ψ_A , ψ_B and ψ_C) are also ignored. Within the complete model, $z(x)$ is calculated via (6) taking into account equations (1)–(5). Thus, in this case χ_{Au} is taken into account in calculating parameters ξ , K , Γ_l , c_l and β_l (these parameters depend on ψ_A , ψ_B and/or ψ_C , and hence on χ_{Au} [27]), which makes the curve $z(x)$ shape differing from that of the curve obtained in the simplified model. Desorption affects (via parameter $I_{A_2}^0$) not only $z(x)$, but also parameter K and, hence, χ_{tot} . Our study has shown that the approximate solution in which a one-parameter equation is used as the liquid–solid dependence provides results close to the complete solution. Deviations are observed only at high temperatures. The paper presents the analysis of the temperature and flux ratio V/III effect on the compositional dependences. Using the example of Au-catalyzed $\text{InP}_x\text{As}_{1-x}$ NWs, we have demonstrated that χ_{Au} does not affect the vapor–solid distribution but does affect χ_{tot} . It is also shown that χ_{tot} is low (in the case of the $\text{InP}_x\text{As}_{1-x}$ NWs, $\chi_{\text{tot}} < 2\%$). The obtained results may be used to optimize the growth parameters of NWs with a preset chemical composition.

Funding

V.G. Dubrovskii expresses his gratitude to the St. Petersburg State University Research Grant (ID 129360164) for financial support of analytical research.

Conflict of interests

The authors declare that they have no conflict of interests.

References

- [1] F. Glas, *Phys. Rev. B*, **74**, 121302 (2006). DOI: 10.1103/PhysRevB.74.121302
- [2] K.A. Dick, P. Caroff, J. Bolinsson, M.E. Messing, J. Johansson, K. Deppert, L.R. Wallenberg, L. Samuelson, *Semicond. Sci. Technol.*, **25**, 024009 (2010). DOI: 10.1088/0268-1242/25/2/024009
- [3] V.G. Dubrovskii, T. Xu, A.D. Alvarez, S.R. Plissard, P. Caroff, F. Glas, B. Grandidier, *Nano Lett.*, **15**, 5580 (2015). DOI: 10.1021/acs.nanolett.5b02226
- [4] E.S. Koivusalo, T.V. Hakkarainen, M.D. Guina, V.G. Dubrovskii, *Nano Lett.*, **17**, 5350 (2017). DOI: 10.1021/acs.nanolett.7b01766
- [5] X. Yuan, D. Pan, Y. Zhou, X. Zhang, K. Peng, B. Zhao, M. Deng, J. He, H.H. Tan, C. Jagadish, *Appl. Phys. Rev.*, **8**, 021302 (2021). DOI: 10.1063/5.0044706
- [6] J. Wallentin, M.T. Borgström, *J. Mater. Res.*, **26**, 2142 (2011). DOI: 10.1557/jmr.2011.214
- [7] B.D. Liu, J. Li, W.J. Yang, X.L. Zhang, X. Jiang, Y. Bando, *Small*, **13**, 170199 (2017). DOI: 10.1002/sml.201701998
- [8] R.S. Wagner, W.C. Ellis, *Appl. Phys. Lett.*, **4**, 89 (1964). DOI: 10.1063/1.1753975
- [9] P. Krogstrup, R. Popovitz-Biro, E. Johnson, M.H. Madsen, J. Nygård, H. Shtrikman, *Nano Lett.*, **10**, 4475 (2010). DOI: 10.1021/nl102308k
- [10] P. Caroff, M.E. Messing, M. Borg, K.A. Dick, K. Deppert, L.E. Wernersson, *Nanotechnology*, **20**, 495606 (2009). DOI: 10.1088/0957-4484/20/49/495606
- [11] F. Jabeen, S. Rubini, F. Martelli, *Microelectron. J.*, **40**, 442 (2009). DOI: 10.1016/j.mejo.2008.06.001
- [12] M. Ghasemi, E.D. Leshchenko, J. Johansson, *Nanotechnology*, **32**, 072001 (2021). DOI: 10.1088/1361-6528/abc3e2
- [13] E. Barrigon, M. Heurlin, Z. Bi, B. Monemar, L. Samuelson, *Chem. Rev.*, **119**, 9170 (2019). DOI: 10.1021/acs.chemrev.9b00075
- [14] E.D. Leshchenko, V.G. Dubrovskii, *Nanomaterials*, **13**, 1659 (2023). DOI: 10.3390/nano13101659
- [15] G. Priante, F. Glas, G. Patriarche, K. Pantzas, F. Oehler, J.-C. Harmand, *Nano Lett.*, **16**, 1917 (2016). DOI: 10.1021/acs.nanolett.5b05121
- [16] V.G. Dubrovskii, A.A. Koryakin, N.V. Sibirev, *Mater. Des.*, **132**, 400 (2017). DOI: 10.1016/j.matdes.2017.07.012
- [17] J. Johansson, M. Ghasemi, *Phys. Rev. Mater.*, **1**, 040401 (2017). DOI: 10.1103/PhysRevMaterials.1.040401
- [18] R. Sjökvist, D. Jacobsson, M. Tornberg, R. Wallenberg, E.D. Leshchenko, J. Johansson, K.A. Dick, *J. Phys. Chem. Lett.*, **12**, 7590 (2021). DOI: 10.1021/acs.jpcclett.1c02121
- [19] D. McLean, *Grain boundaries in metals* (Oxford University Press, N.Y., 1957).
- [20] V.G. Dubrovskii, E.D. Leshchenko, *Phys. Rev. Mater.*, **7**, 074603 (2023). DOI: 10.1103/PhysRevMaterials.7.074603
- [21] V.G. Dubrovskii, *Phys. Rev. Mater.*, **7**, 096001 (2023). DOI: 10.1103/PhysRevMaterials.7.096001
- [22] V.G. Dubrovskii, *Nanomaterials*, **14**, 207 (2024). DOI: 10.3390/nano14020207
- [23] V.G. Dubrovskii, E.D. Leshchenko, *Nanomaterials*, **14**, 1333 (2024). DOI: 10.3390/nano14161333
- [24] E.D. Leshchenko, M. Ghasemi, V.G. Dubrovskii, J. Johansson, *CrystEngComm*, **20**, 1649 (2018). DOI: 10.1039/C7CE02201H
- [25] A.I. Persson, M.T. Björk, S. Jeppesen, J.B. Wagner, L.R. Wallenberg, L. Samuelson, *Nano Lett.*, **6**, 403 (2006). DOI: 10.1021/nl052181e
- [26] B.M. Borg, K.A. Dick, J. Eymery, L.-E. Wernersson, *Appl. Phys. Lett.*, **98**, 113104 (2011). DOI: 10.1063/1.3566980
- [27] E.D. Leshchenko, V.G. Dubrovskii, *Nanotechnology*, **34**, 065602 (2023). DOI: 10.1088/1361-6528/aca1c9

Translated by EgoTranslating